Design Principles and Implementation of Acceleration Feedback to Improve Performance of DC Drives

Peter B. Schmidt Robert D. Lorenz
University of Wisconsin-Madison
Madison, Wisconsin, 53706

Abstract

The objective of this work is to demonstrate the principles, design methodologies, and implementation of acceleration feedback to substantially improve the performance of DC servo drives. The impetus behind this work is the need to improve the stiffness of drives used in motion control applications where load fluctuations cause unacceptable motion errors. Such applications dominate the robotics field as well as many manufacturing processes. To achieve lower amplitudes of load-induced motion errors implies achieving a basic improvement in stiffness. Rather than attempting to improve stiffness by the classical approach of using higher velocity and position state feedback gains (and correspondingly higher bandwidths) this paper demonstrates the fact that acceleration feedback allows substantially higher overall stiffness without requiring higher bandwidths of the velocity and position loops. The paper introduces the fact that acceleration feedback acts as an "active inertia" which acts to produce the higher stiffness. The paper develops these underlying principles in a straightforward manner and demonstrates the performance via both simulation and experiments on two DC drive test systems. This paper distinguishes itself from others using acceleration feedback in two regards: first, the explanation it provides of underlying principles and second, the implementation of acceleration estimation via observers which do not require differentiation of position or velocity feedback signals.

Introduction

Acceleration feedback has been recognized by previous investigators to improve system performance[1-3]. In general, prior work has not clearly demonstrated the fundamental principles of acceleration feedback and has not resolved the issue of how the acceleration feedback signal is reliably obtained using modern, digital drive technology. The primary objective of this paper is to demonstrate both the fundamental principles and the practical implementation of acceleration feedback, including experimental demonstration on the DC drive test systems.

The fundamental principles to be demonstrated include the relationship of acceleration feedback to classical position, velocity, and current feedback, and the unique role of acceleration feedback in providing the equivalent effect of an "electronic" gear reduction. This analogy seems particularly well suited since, unlike the other conventional feedback signals, acceleration feedback will be shown to improve drive stiffness without requiring increased bandwidth on the traditional loops. This is the same affect as a mechanical gear reduction.

For practical implementation of acceleration feedback, a reliable acceleration signal must be obtained economically. This poses two problems. The first problem is that few angular acceleration transducers exist and/or are economical. The second problem is that drive developers would prefer to use only one feedback transducer, which generally will be the optical encoder or the electromagnetic resolver. Thus, the acceleration signal must be derived from a position signal. Prior researchers have implemented differentiation schemes[1-3]. Often these schemes have been based on the assumption of a differentiation of a low noise velocity signal rather than a position feedback signal[1-2]. In general, differentiation techniques are known to produce noisy signals which are severe when using a single differentiation (ie. differentiating velocity) and extremely severe using double differentiation (ie. differentiating position feedback)[3]. Passing these signals through filters adds phase delay which further degrades the signal and limits the performance of the closed loop. To obtain acceleration signals without differentiation requires the use of observers. One such topology is the implementation presented in this paper.

In the following sections, this paper develops the basic theory behind acceleration feedback. It will explain the first principles on what acceleration feedback is, and why it improves the system performance compared to conventional position-, velocity-, and current- feedback techniques. The methodology for designing an observer to generate both a velocity and an acceleration signal will be presented. Following the design, analysis, and simulation of the acceleration feedback, experimental results will demonstrate the benefits and improved performance with acceleration feedback on a two axis DC drive test system and an articulated robot.

Conventional Controller Limitations

The act of providing restoring torques to attenuate motion error response to process disturbances is equivalent to providing dynamic stiffness. From a state controller perspective this is achieved via the

90/CH 2935-5/90/0000-0422$01.00©1990 IEEE

"stiffness" gain on position feedback and the "damping" gain on velocity feedback [1]. Fig. 1 shows the block diagram of such a state feedback controller added in a cascaded configuration with a wide bandwidth current regulating loop typical of modern DC and AC servo drives.

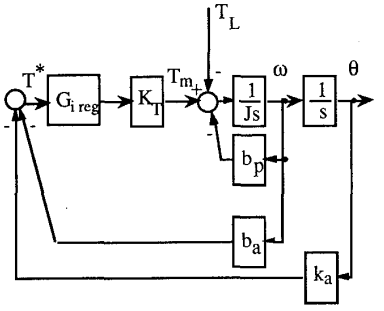

Figure 1 Position and Velocity State Feedback using a DC Motor and Amplifier System with a Cascade Current Regulating Loop for Direct Torque Control

Use of such current regulating loops has proven particularly useful in that it allows direct torque control of the motor. For such systems, the dynamic stiffness is comprised of both passive and active stiffness. The passive stiffness in this system is based on the plant inertia and damping. Active stiffness is added by the damping term and stiffness term resulting from the state feedback gains. The transfer function of the dynamic stiffness for this system is

$$\text{Dynamic Stiffness} = \frac{T_L}{\theta} = J s^2 + (b_a+b_p)s + k_a \qquad (1)$$

The current regulator gain and the torque gain are assumed to be equal to unity. From the location of the controller state feedback gains (b_a and k_a), it is apparent that they act in parallel to any passive mechanical damping (b_p). Because of this parallelism, the controller active gains have the same dimensional units as the physical passive terms for stiffness and damping. Thus, in Fig. 2, the upper curve demonstrates the added effect of additional process damping and stiffness as provided actively by the velocity and position feedback controller. From this diagram, it should be apparent that the dynamic stiffness frequency response is shaped by the active state feedback gains, (b_a and k_a), of the controller. Thus, the motor/amplifier/current regulator is being actively used to reduce the response of the system to process disturbances. It should be noted however, that increasing stiffness or damping gains implies higher bandwidths are required. This is shown in the frequency response function domain via the intersections of the asymptotic line segments which indicate the various bandwidths of the closed loop servo, ie., the velocity loop bandwidth and the position loop bandwidth. The high bandwidths required may not be realizable due to other system limits such as control processor sample frequency limits.

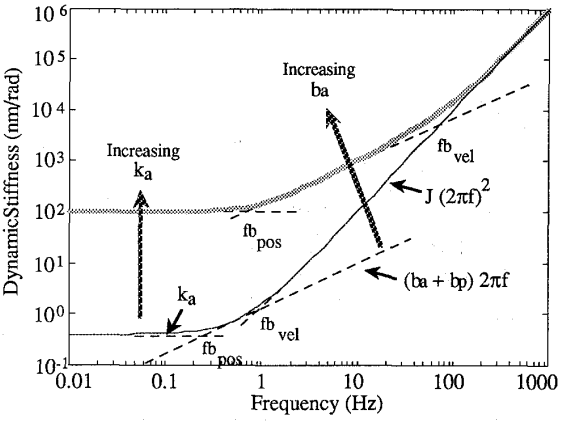

Figure 2 Dynamic Stiffness Frequency Response for a DC Position and Velocity Servo

The controller configuration of Fig. 1 was drawn to emphasize disturbance response properties. Fig. 3 shows the system to which the normal commanded velocity, ω^*, and command position, θ^*, have been added. In this form, the command inputs act as "virtual

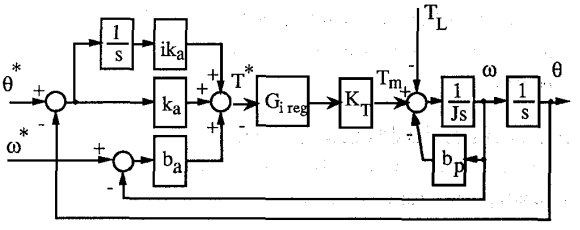

Figure 3 Velocity, Position, and Integrated Position Error State Feedback using a DC Motor and Amplifier System with a Cascade Current Regulating Loop for Direct Torque Control

references" from which deviations are to be corrected by the controller. The feedback gains b_a and k_a retain their meaning as active damping and stiffness relative to the desired velocity and position states. In addition to the commanded inputs for velocity and position, the controller also includes an additional controller state, that of integrated position error, $\int\theta_{error}\,dt$. The commanded value of this state is always zero, ie. no accumulated error is desired. This additional controller state assures that no steady state position error is present if constant disturbances (steady state loads) are present. Since steady state loads are common, this additional state is often advantageously applied. The gain associated with this feedback loop will be denoted as ik_a, which is the integral of stiffness. The dynamic stiffness frequency response effect of this additional state is shown in Fig. 4. The effect of this state integrator is indeed to improve static stiffness to a near infinite value because the full motor torque will be developed if any error (the least significant bit) is present.

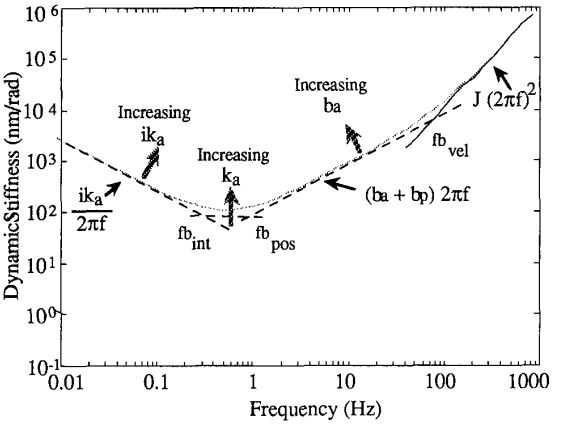

Figure 4 Dynamic Stiffness Frequency Response for a DC Position and Velocity Servo with an Integrated Position Error State, $\int\theta_{error}\,dt$, added to the Controller

It should be concluded that using the classical state feedback terms will increase stiffness only if bandwidth is increased. To raise this entire dynamic stiffness curve will require the use of acceleration feedback.

Acceleration Feedback Principles

Fig. 5 shows a simplified implementation of acceleration feedback, as if acceleration were a readily available feedback signal.

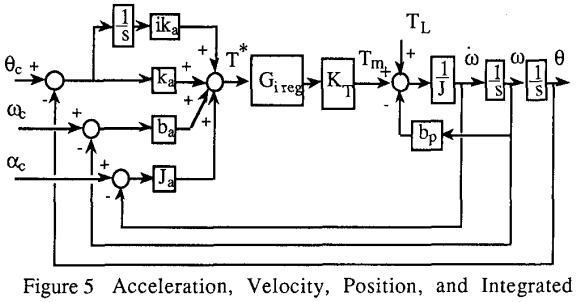

Figure 5 Acceleration, Velocity, Position, and Integrated Position Error State Feedback using a DC Motor and Amplifier System with a Cascade Current Regulating Loop for Direct Torque Control

In this form, the dynamic stiffness equation becomes:

$$\frac{T_L}{\theta} = (J + J_a)\,s^2 + (b_a+b_p)s + k_a + \frac{ik_a}{s} \qquad (2)$$

The effect of acceleration feedback is to introduce the same apparent resistance to disturbance torque as a pure inertia would. This "controller" inertia would make the drive seem like a large flywheel relative to disturbances. The resulting effect on the dynamic stiffness is shown in Fig. 6.

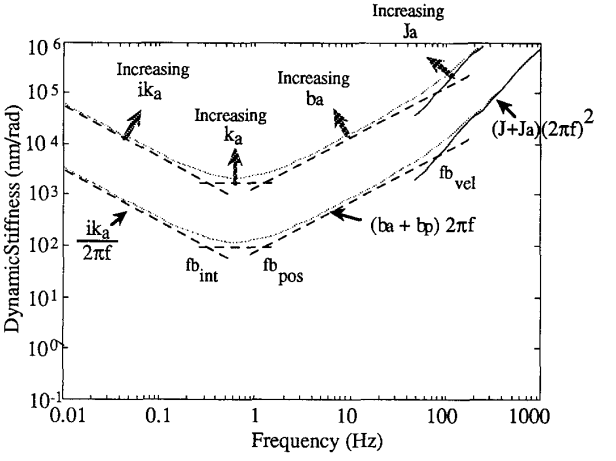

Figure 6 Dynamic Stiffness Frequency Response with Closed Acceleration, Velocity, Position, and Integrated Position Error Loops using a DC Motor and Amplifier System with a Cascade Current Regulating Loop for Direct Torque Control

From Fig. 6, it is apparent that the acceleration feedback has caused the entire stiffness plot to increase without causing an increase in bandwidths. This concept can be understood by comparing the dynamics of the current regulated system with the acceleration feedback system. Fig. 7 is a block diagram of the current regulator cascaded with the velocity and position controller.

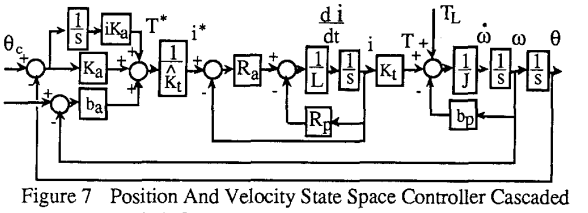

Figure 7 Position And Velocity State Space Controller Cascaded With A Current Regulator

The following assumptions, which are realistic, make the comparison of the two different control schemes easily understood: let $\hat{K}_t \cong K_t$, $b_a >> b_p$ and $R_aJ >> Lb_p$. The transfer function for the dynamic stiffness for this system is

$$\frac{T_L}{\theta} = \frac{JLs^4+J(R_a+R_p)s^3+R_ab_as^2+R_ak_as+R_aik_a}{Ls^2+(R_a+R_p)s} \qquad (3)$$

Fig. 8 is the block diagram of the acceleration feedback loop in parallel with the velocity and position loops.

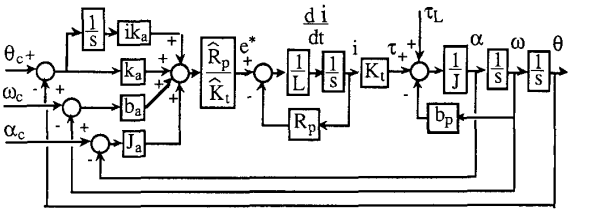

Figure 8 Position, Velocity and Acceleration Feedback Controller

The current loop is no longer closed in this approach. Making the same assumptions as for the current regulated system and the additional assumption $\hat{R}_p \cong R_p$, the transfer function for the dynamic stiffness for this system becomes

$$\frac{T_L}{\theta} = \frac{JLs^4+R_p(J_a+J)s^3+R_pb_as^2+R_pk_as+R_pik_a}{Ls^2+R_ps} \quad (4)$$

Both of these equations can be observed to have equivalent numerators. The numerators are the characteristic equations for the systems. From Fig's 7 and 8, one can observe that the current feedback loop and the acceleration feedback loop act in parallel. The only difference between these two loops in terms of the characteristic equations, are gain values. However, the roots in the denominators of these equations are different, thereby making the acceleration feedback system stiffer in terms of disturbance rejection. A stiffer system is realizable because the acceleration feedback path comes after the disturbance input unlike the current feedback which is before the disturbance. The controller can respond faster because the acceleration feedback signal contains the disturbance torques.

From the previous discussion, it should be apparent that based on fundamental principles, acceleration feedback behaves analogous to a mechanical gear reduction in that the overall stiffness of the DC servo is increased without requiring any change in position or velocity loop bandwidths. Before this model can be applied to practical systems, it is necessary to develop a robust acceleration feedback signal from the position feedback. This will be accomplished via an observer.

An Acceleration Observer

The simplest form of an acceleration observer is to extend the established velocity observer structure for digital position feedback drives[7]. In that form, only a position feedback signal was available for measurement and it acted as a command input to the closed loop observer while the current (torque) input to the drive acted as the command feedforward input. The error between the actual position and the estimated position drove the observer to produce an accurate estimate for the velocity. This velocity observer structure is one part of the acceleration observer shown in Fig. 9.

A similar design approach has been followed to generate an estimate of the acceleration. The actual current (torque) input acts as the feedforward command to both observers. The actual measured position and the velocity estimate from the first observer act as command inputs to the acceleration observer. The observer gains help to force the acceleration signal to track the actual drive. This topology may be reduced algebraically to a simpler form, but the diagrammed form is particularly easy to tune based on the same design criterion used for the actual feedback controller. The bandwidths of the observers and the controlled system are similarly limited by the sample rate of the control computer.

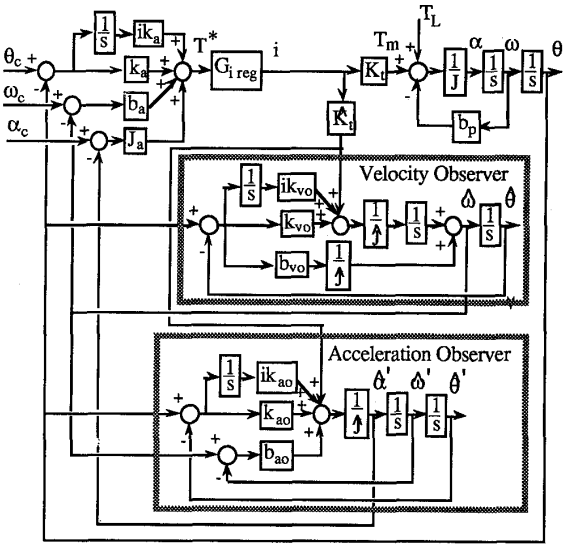

Figure 9 Velocity And Acceleration Observer Block Diagram

Experimental System Implementation and Results

The design of the velocity and acceleration observer was implemented on a Macintosh II with a 68020 microprocessor as the control computer. It had a 68881 floating point coprocessor and 8 Megabytes of RAM. The control and observer algorithms were written utilizing the Lightspeed C programming language. The data acquisition/control interface system was based on a GW Instruments MacADIOS motherboard that plugged into the NuBus backplane. This board, along with daughter cards, allowed A/D and D/A conversions to take place between the controller and the motors. A programmable gate array designed by XILINX was utilized to convert the incremental optical encoder quadrature channel pulses into a digital absolute position.

The control algorithm was tested on two systems. The first test system was comprised of two EG&G DC permanent magnet motors. Each motor had a current regulator based on a linear amplifier. The analog output from the control computer provided a current command to the drives. The two motors were directly coupled together. One motor acted as the control motor, while the second motor could be commanded to act as a programmable load. The test configuration can be seen in Fig. 10.

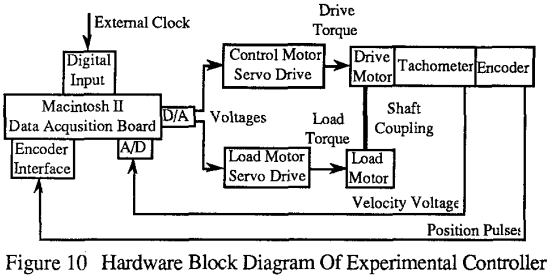

Figure 10 Hardware Block Diagram Of Experimental Controller and DC Drive Test Setup

Various tests were conducted with and without the acceleration observer in place. The actual velocity signal as measured by a DC tachometer was utilized as a reference for comparing the performance of the different systems. One test that was conducted on this system was to command the control motor to turn with a constant velocity of 10 revolutions per second. The programmable load introduced a disturbance of 0.77 Newton-meters at a frequency of 10 Hertz. Fig. 11 is a comparison of the velocity signal of the motor with and without acceleration feedback.

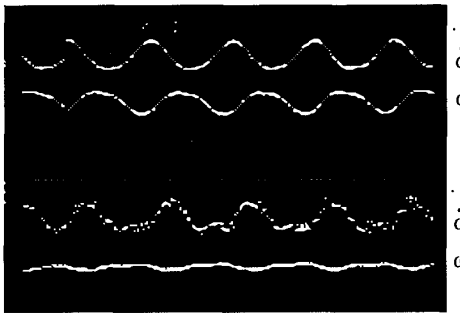

All Vertical Scales $5.0 \frac{volts}{div}$ All Horizontal Scales $50 \frac{msecs}{div}$

Velocity Input Command: $10 \frac{revs}{sec}$, DC
Load Disturbance Command: 0.77 N-m, 10 Hz AC

Figure 11 Comparison of Disturbance Rejection With and Without Acceleration Feedback

The top two oscilloscope traces are the manipulated acceleration input and the motor velocity without acceleration feedback. From the velocity plot, one can observe the load disturbance present in the feedback signal. The bottom two traces are the same signals with acceleration feedback. The addition of acceleration feedback has notably reduced the amount of load torque disturbance in the velocity signal.

The previous test was repeated to make a comparison between the current-velocity feedback controller and the current-velocity-acceleration controller over a wide range of frequencies. The test motor was commanded to rotate at a constant velocity. The torque command input to the load motor was random noise. Fig. 12 is a digitized plot of the output from the spectrum analyzer. The data on the graph is the magnitude ratio of the load disturbance over the test motor velocity. The circled (o) points are from the controller with only the current loop closed. The only damping in this system is due to the inertia of the motor and load. The circled data is a fairly straight line increasing at 20 dB per decade. The plus (+) points are generated from closing the current and velocity loops. The figure demonstrates the addition of the active damping in the system by the horizontal line at the lower frequencies. The starred (*) data is attributed to the current, velocity and acceleration loops simultaneously being closed. Closing the acceleration loop increases the apparent system damping between 3 and 70 Hz approximately.

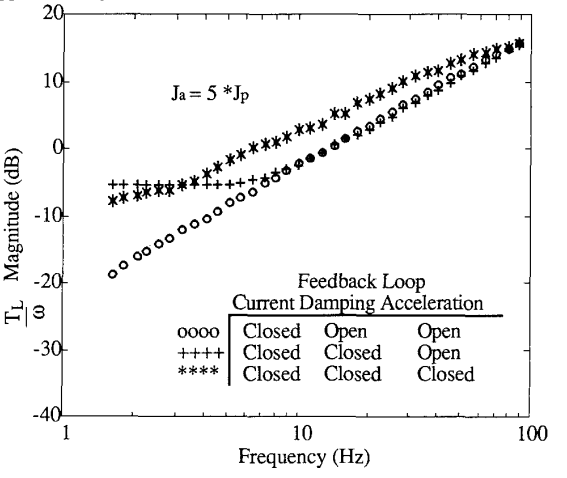

Velocity Input Command: $6 \frac{revs}{sec}$ @ DC
Load Disturbance Command: random noise

Figure 12 Frequency Analysis Of Disturbance Rejection With and Without Acceleration Feedback

The second test stand couples the control computer utilized in the first system with a Puma controller and robotic manipulator. The Puma controller is an LSI-11 based system which utilizes a Q-bus backplane and has its own operating language. The robot is a six degree of freedom articulated manipulator. The closed form and proprietary nature of the robot controller necessitated a special interface to be designed to be able to test various control strategies. A hardware block diagram of the interface to the Puma robot controller can be seen in Fig. 13.

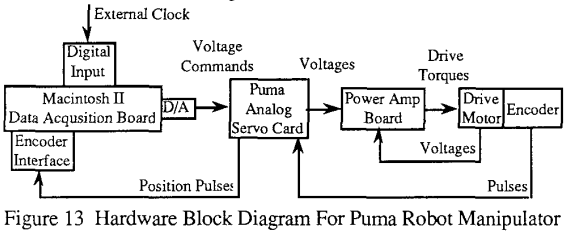

Figure 13 Hardware Block Diagram For Puma Robot Manipulator

The robot was tested to observe the effects of acceleration feedback on one of the joints. The velocity and acceleration profiles in joint space are generally very complicated when executing a dynamic trajectory. Therefore, joints one and two were commanded to remain fixed at a stationary point. Joint three was programmed to cycle between +/- 5 degrees at a rate of 90 degrees per second. As joint three accelerates, it causes an equal magnitude and opposite direction torque to be applied to joint two.

Fig. 14 contains oscilloscope traces for joint two. The top two traces are the joint velocity and torque command respectively when

the active inertia gain is zero. The plot demonstrates how joint two rotates and the torque command tries to create an equal but opposite torque to cancel the change in velocity. The bottom two traces reflect the actions of the controller when there is acceleration feedback. The joint displacement is less when there is acceleration feedback.

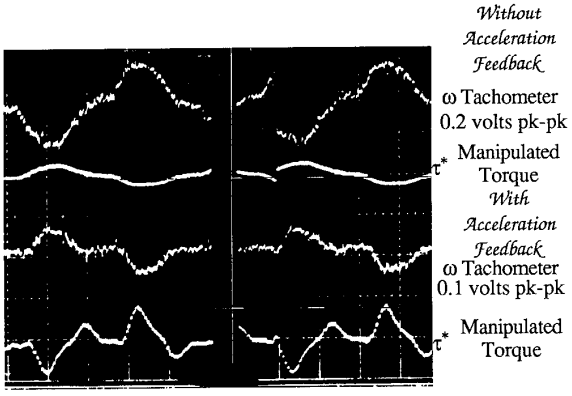

Figure 14 Joint 2 Disturbance Rejection Utilizing Acceleration Feedback

The nonlinear coupling torques acting on a robot joint can be modeled as load disturbances. These disturbances can be rejected by applying acceleration feedback. Modeling each joint as a second order system with load disturbances, enables a simple straight-forward control scheme to be implemented.

Conclusions

This paper has developed the first principles of acceleration feedback and design methods for its practical implementation.

The first principles have shown that:

- Acceleration feedback increases the effective inertia of the system for disturbance rejection purposes. This allows higher overall stiffness to be achieved without increasing position and velocity loop bandwidths. The effect is analogous to an electronic gear reduction.
- Acceleration feedback acts in parallel to current feedback. However, unlike current feedback, acceleration feedback acts to improve disturbance rejection. Thus acceleration feedback is advantageously applied for disturbance-driven servo applications such as robot motion controls.

The design methodologies developed in this work have shown that:

- Acceleration feedback can be implemented with only the position transducer already being utilized for feedback.
- Acceleration feedback can be obtained without need for differentiation of signals by using appropriate observers.
- Accelertion observer topologies which lend themselves to ease of design and interpretation include parallel configurations.

The experimental results have demonstrated that

- The developed principles operate as expected to reduce disturbance response.
- Limits in utilizing acceleration feedback generally arise due to limits in the sample rate of the controller and observer implementation. This is because the bandwidth of the observer is very directly related to this sample rate limit.
- Reducing or eliminating the current loop will increase the acceleration feedback gains (ie., the active inertia) but the inherent protection provided by current limits is no longer present and must be replaced by other approaches.

Acknowledgement

The authors wish to acknowledge the motivation and partial financial support and provided by the Wisconsin Manufacturing Automation and Robotics Consortium (WMARC) and the Wisconsin Electric Machines and Power Electronics Consortium (WEMPEC) of the the University of Wisconsin-Madison and by the Allen-Bradley Company of Milwaukee, Wisconsin.

References

1. Hori, Y., Disturbance Suppression On An Acceleration Control Type DC Servo System, *Conf. Record PESC,* 1988, pp. 222-229.
2. Hori, Y., Position And Mechanical Impedance Control Method Of Robot Actuators Based On The Acceleration Control, *Conf. Record PESC*, 1989, pp. 423-430.
3. Ohishi, K., Matsuda, S., Ohnishi, K., DSP-Based DC Servo Acceleration Control Without Speed Sensor, *Conf Record of IEEE, IAS Annual Meeting*, San Diego, 1989, pp. 480-485.
4. R. D. Lorenz, P. B. Schmidt, "Synchronized Motion Control for Process Automation",*Conf Record of IEEE, IAS Annual Meeting*, 1989, pp. 1693-1698.
5. R. D. Lorenz, "Synthesis of State Variable Controllers for Industrial Servo Drives", *Proceedings of the Conf. on Applied Motion Control*, June, 1986, pp. 247-251.
6. R. D. Lorenz, M. O. Lucas, D. B. Lawson, "Synthesis of a State Variable Motion Controller for High Performance Field Oriented Induction Machine Drives", *Conf Record of IEEE, IAS Annual Meeting*, 1986, pp. 80-85.
7. R. D. Lorenz and K. Van Patten, "High Resolution Velocity Estimation for All Digital, AC Servo Drives", R. D. Lorenz and K. Van Patten, *Conf Record of IEEE, IAS Annual Meeting*, 1988, pp. 363-368.